JTTEE5 7:197-204

PEER REVIEWED

Investigation of Alumina Splats Formed in the Induction Plasma Process

X. Fan, F. Gitzhofer, and M. Boulos

(Submitted 20 April 1997; in revised form 14 October 1997)

The investigation of the flattening behavior of Al_2O_3 particles melted in the induction plasma process was reported. Three typical morphologies of alumina splats were recognized: mushroom-like, pancake-like, and flower-like types. Through the conduct of a 2^4 factorial design of experiments, it was determined that the important factors controlling the deformation of splats are the pressure in the spray chamber, the spraying distance, and the powder size. Interactions among these three factors are significant. Using plasma diagnostic techniques, the relation between the splat morphology and the surface temperature and velocity of particles prior to impingement on the substrate was established.

Keywords alumina splat, design of experiment, induction plasma process

1. Introduction

The aim of plasma spraying is the production of coatings or structural parts of various materials by "piling" up particles on a substrate or mandrel. An understanding of the deformation behavior and the solidification of individual particles will lead to the modeling and control of the processing parameters which govern the resulting "splat" characteristics. This ultimately permits the production of spayed materials with optimized and/or desired properties. Until the end of the 1990s, there were few publications on this subject (Ref 1-6), despite the existence of many splat photos published in articles on plasma spraying. Research described data more related to plasma/particle in-flight interactions and plasma parameters/coating microstructure studies. In the past several years, however, an abundance of "splat forming" research studies has surfaced (Ref 7-19), with the implication that more attention has been focused on the droplet/substrate interactions taking place during thermal spray processing.

Notable early works include the study by Madejski on the solidification of a droplet on a cold surface (Ref 1). In his proposed model, a sprayed droplet, impinging perpendicularly onto the cold substrate surface, flattens to form a cylinder. The phenomena of solidification and the free flow of material are considered simultaneously. The subsequent formation of the splat starts from a cylindrically shaped liquid droplet, which possesses kinetic and thermal energies. The droplet develops into a regular round disk until the material is totally solidified. Using the concept of conservation of energy (kinetic, potential, and the work expended in overcoming friction forces), the expression for the derivative dR/dt (the differential coefficient of the splat radius with respect to time) was derived. Thus, it is possible to estimate the dimension of the splat produced from the initial droplet parameters with the aid of numerical techniques. The Madejski model, expressed in Eq 1, has been widely cited:

$$D/d = 1.294(Re)^{0.2} \quad \text{(Eq 1)}$$

where D/d is the ratio of the average flattened particle diameter to the average initial particle diameter and Re is the Reynolds number.

Recent research on "splat forming" in plasma processes has produced some important results. First, it has been recognized that the substrate temperature plays an important role in determining both the morphology and the dimensions of the splats (Ref 8, 9, 11). Second, both theoretical simulation and experimental observations by the Yoshida group (Ref 6, 7, 10) have indicated that the droplets formed from many materials only begin to solidify at the end of deformation; that is, the deformation continues until the end of material spreading and loss of all kinematic energy and does not depend on the solidification step. This observation has been further confirmed for low Re value cases by research work at the University of Toronto (Ref 12, 15, 17).

A study of Al_2O_3 particle splats formed in the induction plasma spray process is described in this paper. Three typical morphologies of alumina splats have been distinguished: mushroom-like, pancake-like, and flower-like types. A 2^4 factorial experimental design has determined the main parameters influencing the deformation of melted particle droplets in the induction plasma process. With the help of plasma diagnostic techniques, the relationship between the splat morphology and the surface temperature and velocity of particles prior to impingement on the substrate has been established.

2. Alumina Splats Forming in the Induction Plasma Process

2.1 Alumina Splats Morphologies

A schematic of the experimental setup used for the study of induction plasma splat forming is presented in Fig. 1. It consists of a high energy density plasma torch, a powder injection probe,

X. Fan, F. Gitzhofer, and **M. Boulos,** Plasma Technology Research Center, University of Sherbrooke, Sherbrooke, Québec J1K 2R1, Canada. X. Fan is presently with National Institute for Research in Inorganic Materials (NIRIM), Namiki 1-1, Tsukuba, Ibaraki 305, Japan.

a substrate support, and a water-cooled chamber which is connected to the spray exhaust system. The induction torch was operated under the conditions listed in Table 1. To obtain individual particle splats, the substrate was shielded by a pneumatically activated mask (not shown in Fig. 1) until the commencement of the spray exposure period, so that sampling of individual splats was possible.

Three broad types of alumina splat morphologies have been identified as being formed in the induction plasma spraying process: mushroom-like, pancake-like, and flower-like.

Figure 2 illustrates splats produced having a mushroom-like shape. Splats of this type were generated with the use of Al_2O_3 particles that were of an average particle size, *dp*, of 63.4 μm, and a standard deviation, σ, of 8.5 μm, at the 25 kW torch power level, and at a spray chamber pressure of 350 torr (1 torr = 0.133 kPa). The shape of this type of splat reflects insufficiency of particle melting in the spraying process. The material from the outer regions of the particles which is fully molten after traversing the plasma plume, is spread over the substrate as a splat and surrounds the unmelted particle core. In comparison to the situation in the direct current (*dc*) plasma spray process, the unmelted solid cores are retained in the centers of splats produced by induction plasma process, rather than "bouncing off" the substrate. This is a salient feature of the induction plasma process and reflects the relatively low impact velocity of melt particles produced by that process.

Figure 3 illustrates splats of the pancake-like type generated under the same conditions as indicated in Fig. 2 but using a smaller size (dp = 48.0 μm, σ = 12.0 μm) of particles and a relatively higher chamber pressure (500 torr). The pancake-like type form presents a uniform, flat, and smooth surface of an almost perfect circular circumference. A depression is also observed at the center of the splats. The production of such splats confirms that, under appropriate spraying conditions, it is possible to fully melt and splat low momentum alumina particles in an induction plasma process. As well, liquid oxides have much lower surface energies and higher specific heats than solid metals (Ref 20), and consequently, sprayed oxide layers tend to wet their metal substrates with contact angles varying between 0 and 50°. This is shown in Fig. 3, where full wetting of the metal substrate by the alumina splats has taken place.

Figure 4 illustrates splats of the flower-like type. The droplet material splashed and was jetted away from the point of impact on the substrate. This type of splat is obtained under the same conditions as indicated in Fig. 3 but using a relatively long spraying distance, Z_s, of 32 cm. The substrate temperature for this condition is believed to be less than in the case where Z_s = 20 cm. The observation regarding the spray distance variation of

Table 1 Summary of the induction plasma operating conditions

Torch TEKNA PL50 (Tekna Plasma Systems Inc., Quebec, Canada)
Plasma gas flow rates, L/min
Plasma gas: Ar 44
Sheath gas: Ar 90 + H_2 9.6
Oscillator frequency: 3 MHz
Plate power: 25 kW

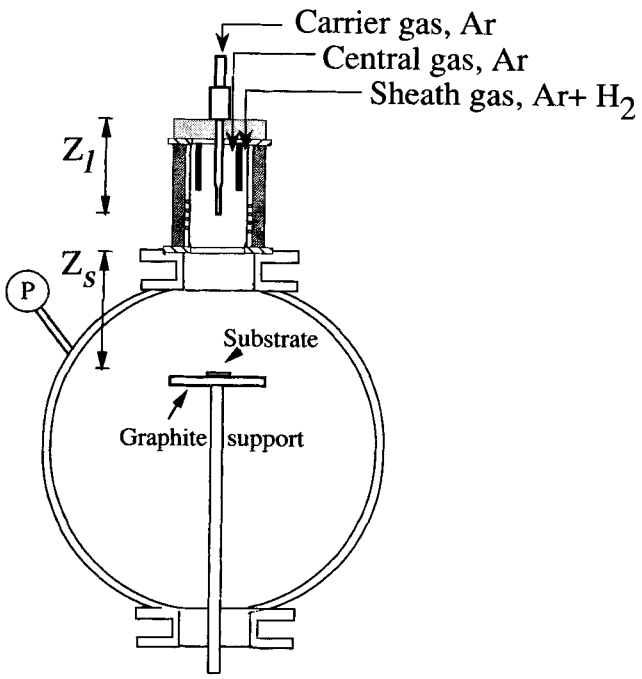

Fig. 1 Schematic of experiment setup

Fig. 2 Mushroom-like type of splats. Al_2O_3 powder of d_p = 63.4 μm, σ = 8.5 μm, 25 kW, 350 torr, Z_1 = 17 cm and Z_s = 20 cm

splat morphology conforms with the phenomena reported by Bianchi et al. (Ref 9, 11) and Fukumoto et al. (Ref 18, 19). Further investigation of the particle parameters reveals that the origin of this kind of splat may result from either particle melt superheat or excessive velocity of droplets at impact.

2.2 The Design of Experiments and Results

This statistical study was to verify the overall trends on the splat shape sensitivity to spraying conditions. Factorial experiment design, which identifies the effects, especially joint effects, of various factors on the measured response, is particularly suitable for the investigation of the induction plasma spraying process, where a large number of parameters are likely to be involved. The factorial design of the experimental series (Ref 21) was used to study the alumina splats formed by the induction plasma process. On the basis of results from a previous statistical study on alumina particle spheroidization (Ref 22), the following factors were chosen for a series of splat forming spray experiments of 2^4 factorial design:

- Factor A: flow rate of carrier gas, Q_1
- Factor B: pressure in the spray chamber, P
- Factor C: spraying distance, Z_s
- Factor D: particle size, dp

These four factors were expected to influence the injected particle momentum, its plasma residence time, and the heat exchange phenomena in the plasma. Two levels were assigned to each factor. The temperature of the substrate was not selected as an independent factor because of the technical difficulty of temperature measurement in the radio frequency environment. However, the influence of this factor may be partly and indirectly reflected in the variation of the spraying distance, Z_s. The variation of pressure in the spray chamber may also induce some change in substrate temperatures. The influence arising from the substrate temperature in these experiments is confounded from the statistical viewpoint with that of other selected factors. Other important factors which influence particle melting and deformation behavior, such as plasma power, plasma gas composition, and flow rate, were held constant during the experiment; see Table 1. Among the reasons for selecting fixed value parameters are the following: the inductively coupled plasma torch has an optimum working range, and the four factors selected are actual process-related parameters, rather than equipment-related parameters.

Previously, the spheroidization of alumina particles in the induction plasma process (Ref 22) determined that the lower injector position provides the most satisfactory yield of melted particles at the moderate powder feed rate (10 g/min). Therefore, the injector

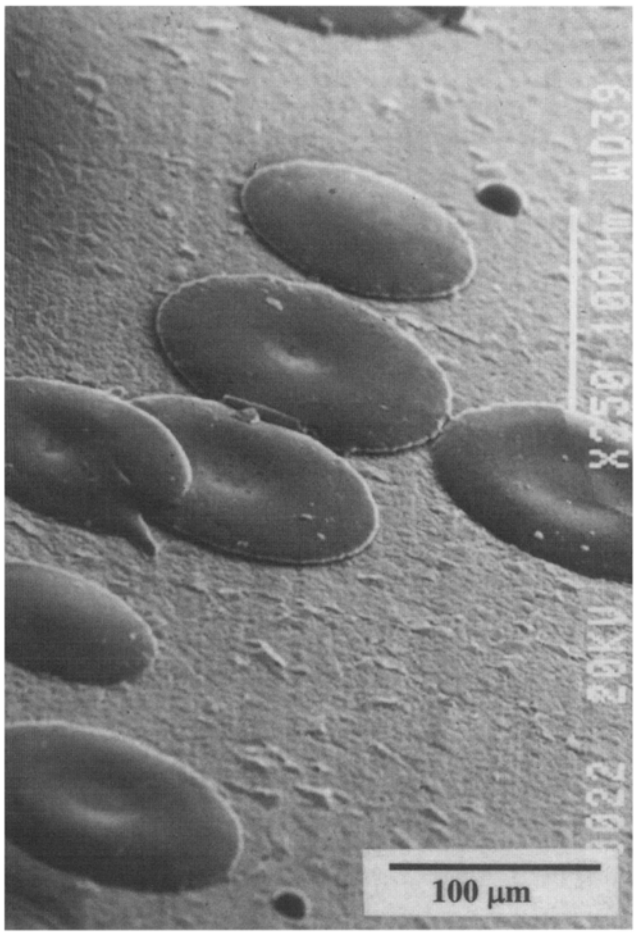

Fig. 3 Pancake-like type of splats. Al_2O_3 powder of d_p = 48.0 μm, σ = 12.0 μm, 25 kW, 500 torr, Z_1 = 17 cm and Z_s = 20 cm

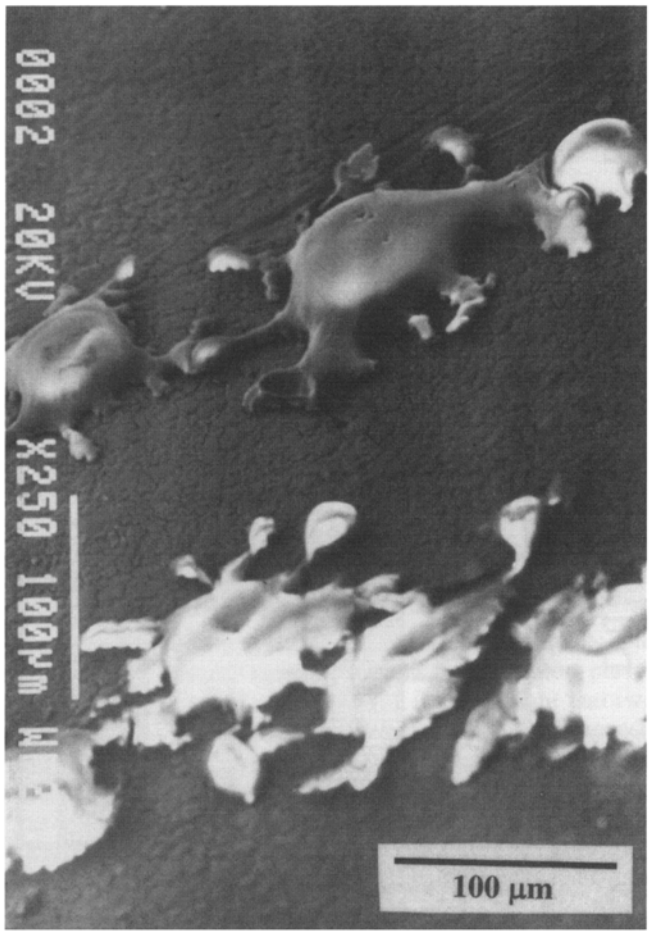

Fig. 4 Flower-like type of splats. Al_2O_3 powder of d_p = 48.0 μm, σ = 12.0 μm, 25 kW, 500 torr, Z_1 = 17 cm and Z_s = 32 cm

position in this series of experiments was fixed at $Z_1 = 17$ cm. The necessity to observe individual splats and the limitations of the sampling techniques led to the Al_2O_3 powder feed rate being fixed at the low value of 3 to 5 g/min in this series of experiments involving only short spray periods.

The substrates used to receive the spray deposit in this study were stainless steel disks, 25.4 mm in diameter and 5 mm in thickness, and were placed on graphite supports. The mean diameters of the flattened particles were measured from optical microscopic views of splat samples (approximately 100 to 150 splats counting for each sample). Results are listed in Table 2. Figure 5 illustrates the responses with respect to the factors that were studied.

2.3 *Statistical Analysis on the Particle Splatting Results*

The particle deformation degree, *D/d*, (the ratio of the average flattened particle diameter to the average initial particle diameter), was used to estimate the effects of the four factors and their interactions. When data were analyzed from factorial design experiments, the effects of the various factors, as well as their interactions, were initially checked by plotting the estimates of the effects as a normal probability graph. This normality check indicated that none of the three- or four-factor interactions had significant influences, so they were combined as an estimate of error. The further corresponding analysis of variance is provided in Table 3.

Through the factorial experiments, the effects of the four selected factors on the particle melt flattening behavior were assessed as follows.

2.3.1 Factor A: the Carrier Gas Flow Rate, Q_1

This factor, within the range of values selected for this series of experiments, appears to have no obvious influence on the droplet flattening behavior.

2.3.2 Factor B: the Pressure in the Spray Chamber, *P*

The pressure in the chamber emerges in this study as the most important factor in the droplet flattening behavior. The influence of pressure in the spray chamber is revealed in two ways: (a) it changes the in-flight particle velocity, and consequently (b) there is a change of residence time for particles in the induction

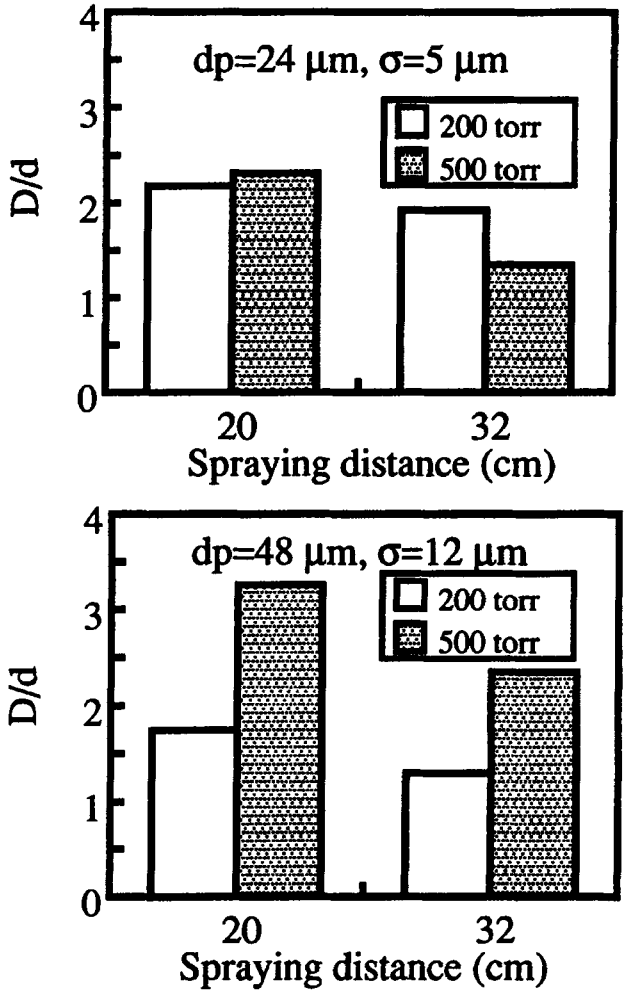

Fig. 5 Alumina particle deformation degree versus the pressure in the chamber, the spraying distance, and particle size

Table 2 Design of splats experiments and results

Treatment combination	Q_1, L/min	P, torr	Z_s, cm	d_p, μm	Average D/d
1	5.5	200	32	48	1.29
a	9.3	200	32	48	1.57
b	5.5	500	32	48	2.35
ab	9.3	500	32	48	2.93
c	5.5	200	20	48	1.74
ac	9.3	200	20	48	1.87
bc	5.5	500	20	48	3.25
abc	9.3	500	20	48	3.33
d	5.5	200	32	24	1.92
ad	9.3	200	32	24	1.88
bd	5.5	500	32	24	1.35
abd	9.3	500	32	24	1.18
cd	5.5	200	20	24	2.18
acd	9.3	200	20	24	1.93
bcd	5.5	500	20	24	2.31
abcd	9.3	500	20	24	2.36

Table 3 ANOVA for splats experiments

Source	Effect	Sum of squares	Degree of freedom	Mean square	F
A	0.076	0.023	1	0.023	<1
B	0.589	1.387	1	1.387	41.04(a)
C	0.564	1.274	1	1.274	37.69(a)
D	0.403	0.649	1	0.649	19.20(a)
AB	0.053	0.011	1	0.011	<1
AC	-0.077	0.024	1	0.024	<1
AD	0.185	0.137	1	0.137	4.05
BC	0.290	0.336	1	0.336	9.94(b)
BD	0.755	2.279	1	2.279	67.43(a)
CD	-0.056	0.013	1	0.013	<1
Error		0.169	5	0.034	
Total		6.302	15		

(a) Significant at 0.01. (b) Significant at 0.05.

plasma, associated with the shift in particle velocity. The first change (a) is related to the particle momentum, and the second change (b) is related to the extent of particle melting. Therefore, the pressure in the chamber significantly influences the flattening behavior.

Further, very intense effects, arising from the interactions between chamber pressure and other factors, are observed. The most important interactions are those of pressure with particle size, BD, and pressure with spraying distance, BC. For example, increasing the chamber pressure augments the *D/d* ratio of the larger particle powder (d_p = 48 μm). For small particles (d_p = 24 μm) at short spraying distances, this augmentation is limited, while at large spraying distances, the ratio actually decreases. See Fig. 5. These observations indicate that the pressure in the spray chamber of the induction plasma process is very important. It should always be optimized with due consideration for all other operating parameters.

2.3.3 Factor C: the Spraying Distance, Z_S

The influence of the spraying distance on the flattening behavior of particles is evident in the *F*-test findings in Table 3. At close spraying distances, droplets retain their molten state to the point of impact on the substrate so that larger *D/d* ratio splats are achieved. If the spraying distance becomes too large, cooler but still soft, or even partially solidified droplets, impinge on the substrate and result in poor flattening behavior and splat formation. Also the substrate temperatures developed at these two levels of Z_S can be different.

2.3.4 Factor D: the Particle Size Distribution, d_p

The mechanism of heating and cooling of particles in a plasma is described through an energy balance by the following hypothesis:

$$Q_T = \pi d_p^2 h_c (T - T_p) - \pi d_p^2 \sigma_s \varepsilon (T_p^4 - T_a^4) \quad \text{(Eq 2)}$$

$$Q_T = \frac{\pi}{6} \rho d_p^3 c_p \frac{dT_p}{dt}; T < T_m \text{ and } T_m < T < T_b \quad \text{(Eq 3)}$$

where Q_T is total heat transfer rate to the particles, d_p is particle diameter, h_c is heat transfer coefficient, c_p is specific heat, T is plasma temperature, T_p is particle temperature, T_m is melting point of particle material, T_b is boiling point of particle material, T_a is ambient temperature, σ_s is Stefan-Boltzmann constant, ε is emissivity of the particle surface, and ρ is density of particle material.

The convective heat transfer occurring between the plasma and injected particles is the principal particle heating mechanism, while the dominant cooling mechanism is that of radiation from the particle surface to the surrounding water-cooled walls of the spray chamber. Equations 2 and 3 show that the change of in-flight particle temperature in the plasma is inversely proportional to the particle diameter.

$$\frac{dT_p}{dt} \propto \frac{1}{d_p} \quad \text{(Eq 4)}$$

This relation predicts how the particle size influences the melting and consolidation behavior of in-flight particles. The statistical analysis recorded in Table 3 verifies that particle size is an important factor in determining the degree of particle deformation.

2.4 Interrelationships among Experimental Factors

From a combination of the experimental data in Table 2 and the analysis of variance in Table 3, the following statistical conclusions are drawn.

Among the four factors selected for study, the spray chamber pressure, *P*, (factor B) appears to be the most important. Thereafter, the spraying distance, Z_S, (factor C) and the initial particle size, d_p, (factor D) also play contributing roles in the splat flattening process.

All of the high-order (≥3) interactions have a negligible effect on the splat flattening behavior. Two-factor interactions are also not very significant except for BC and BD (the chamber pressure and the spraying distance, and the chamber pressure and the powder size). In particular, the interaction BD is very large. The effects of the spraying chamber pressure, when combined with other factors, drastically affect experimental outcomes.

The interaction AD (the carrier gas flow rate and the particle size) is significant only at the 0.25 level, according to *F* statistical analysis. The interactions AB, AC, and CD are not considered significant.

The experimental results in Table 2 indicate that the largest average *D/d* of the powders with d_p = 24.0 μm and d_p = 48.0 μm are 2.36 and 3.33, respectively. These average *D/d* values agree with the data reported by Okada et al. (Ref 23).

The average thickness of splats produced in this series of experiments were estimated as 2.87 μm (for particles of d_p = 48 μm) and 2.94 μm (for particles of d_p = 24 μm). Correspondingly, the ratio of the average thickness to span is ~1 to 20 (for particles of d_p = 24 μm) and ~1 to 50 (for particles of d_p = 48 μm), respectively.

3. The Relationship between Particle Parameters and Splat Morphologies

3.1 Measurement Principles

Simultaneous observations of particle in-flight velocities and particle surface temperatures in the induction plasma spraying process are made through time-of-flight and two-color pyrometer measurements, respectively. The diagnostic technique analyzes a burst of radiation waveforms generated as a hot particle passes across the observation window. As the particle moves, it gives rise to a trapezoidal-shaped light burst which can be captured and analyzed in both its amplitude and time domains. From the analysis, the particle velocity, U_p, can be calculated:

$$U_p = \frac{H}{t_w \cdot \text{IMR}} \quad \text{(Eq 5)}$$

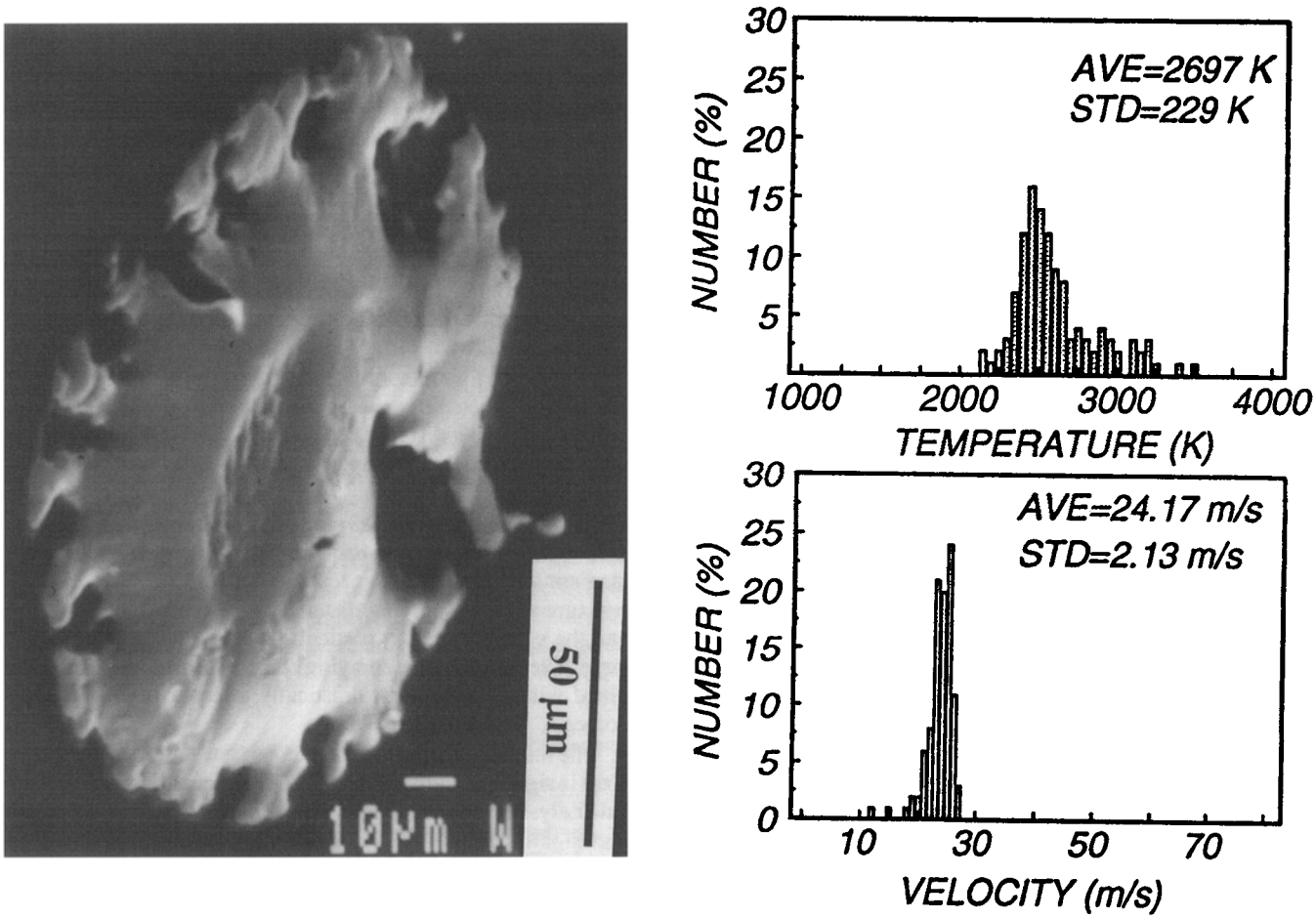

Fig. 6 The flower-like type alumina splat and the corresponding distributions of the particle surface temperature and velocity prior to their impact on the substrate. –75 + 63 μm, 25 kW, 250 torr, Z_t = 22.6 cm

where U_p is the particle velocity, H is the window height, t_w is the burst pulse width, and IMR is the image ratio of the optical setup.

Surface temperatures of particles heated under induction plasma conditions were measured by the two-wavelength pyrometer technique. If the particle behaves as a gray body emitter, the surface temperature, T_p, is determined from the ratio of amplitudes at two distinct wavelengths, λ_1 and λ_2, measured simultaneously, according to Plank's law:

$$T_p = \frac{hc}{k}\frac{(\lambda_1 - \lambda_2)}{\lambda_1\lambda_2} \div \left[\ln\left(\frac{I_{\lambda_1}}{I_{\lambda_2}}\right)^5 \cdot \ln\left(\frac{\lambda_1}{\lambda_2}\right) \right] \quad \text{(Eq 6)}$$

where c is the velocity of light, h and k are the Plank and Boltzmann constants, I is the radiation intensity, respectively.

A specially designed pneumatic device constituted the particle sampling system which was interfaced hermetically to the vacuum chamber. A mirror-like polished stainless steel substrate (2.54 cm in diameter) was installed on the sampling arm. The particle sampling system allowed the capture of particle splats to be performed at the same spatial position where the measurement of the particle in-flight temperature and velocity was performed. Three splat collection positions were chosen in accordance with the available optical access windows on the spray chamber. These were at distances of 11.6, 21.6, and 31.6 cm from the tip of the powder injection probe, denoted as Z_t.

3.2 Particle Parameters and Splat Morphology

To correlate the splat morphology with the T_p and U_p of the precursor droplet, the parameters at the point of collection of the splats have been measured. The observations involved changing some of the spray operating parameters, such as the plasma power, the pressure in chamber, and the spraying distance. Figure 6 illustrates one example of a flower-like splat type obtained at Z_t = 21.6 cm. The corresponding distributions of the T_p and U_p of the droplets, prior to their impact on the substrate, are presented on the right hand side of the micrograph.

A general rule covering the formation of splats was derived from the number of observations of splats with different T_p and U_p values, prior to their impact on the substrate. In Fig. 7, a demarcation of the splat nominal configuration appears, along with their respective T_p and U_p values prior to impact. There is a threshold of T_p and U_p values for the particles form the ideal pancake-like type of splats. Below these threshold values, the droplets lack adequate heat and momentum content for splat formation and remain spherical, or at the extreme retain the original polyhedron form when intercepted by the sampling arm. See zone 1 in Fig. 7. A majority of pancake-like splats will only be produced when the droplets attain $T_p > 2300$ K

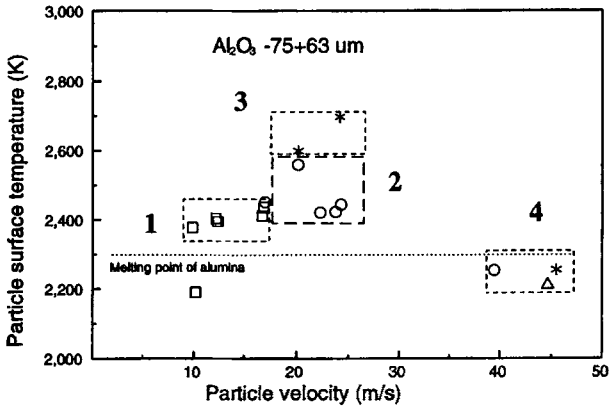

Fig. 7 Correlation between the splats configuration and the particles surface temperature and velocity when particles are impacted on the substrate

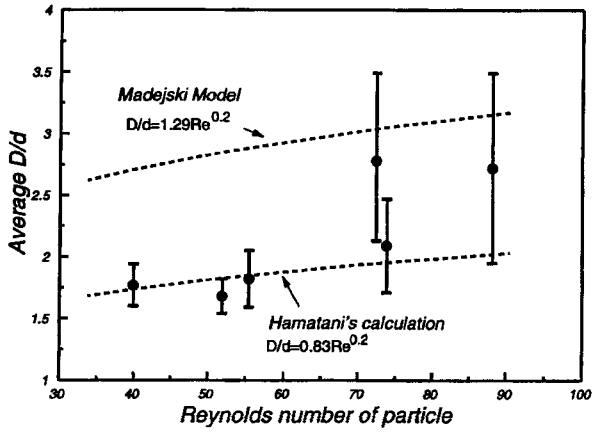

Fig. 8 Comparison of *D/d* between the experimental data and the theoretical models

and $U_p > 20$ m/s (in zone 2). Further increases in T_p (zone 3) lead to flower-like splats. The main reason for this change may be attributed to the diminished viscosity of the liquid state droplets. Lower viscosity favors the spreading of splats on the substrate. In zone 4, the average surface temperatures of droplets are lower than the melting point of alumina, but velocities of these particles are high. In fact, all three kinds of splats have been observed in this region. Those particles may experience plastic deformation to form mushroom and/or pancake morphology splats with their high associated momentum. The high momentum of the molten particles can also result in the melted material jetting away from the impact site, as with random "flower petals" giving rise to the flower-like type of splats.

3.3 Particle Parameters and Splat Dimension

With the measurements of T_p and U_p, the Reynolds number of the melted particles can be estimated and a comparison made of the experimental data with the existing theoretical models that predict the possible degree of particle flattening.

Figure 8 depicts the fit of the model to the experimental results. The measurements are more scattered at higher *Re* values, reflecting the difficulty in controlling individual particle trajectories and their corresponding thermal and kinematic histories in the induction plasma. However, the ascending tendency of deformation degree with the increase of *Re* value is evident. The Madejski formula slightly overestimates the degree of deformation, since that formula is derived for an extreme condition; that is, where the solidification and surface tension are neglected.

Hamatani et al. (Ref 6) also performed "splat form" calculations based on the numerical technique for incompressible fluid flows, and the specified particles of Al_2O_3 in induction plasma process were selected for imitation of the calculation results. In the case of particles of 100 μm in diameter, the formula for the splat form was presented as:

$$D/d = 0.83(Re)^{0.2} \quad \text{(Eq 7)}$$

Their calculation commences from a spherical droplet instead of the cylinder. This can be an important reason for obtaining the better model fit with measured data.

4. Conclusions

The Al_2O_3 splats formed in the induction plasma process exhibit three types of configurations: mushroom-like, pancake-like, and flower-like types. The first two configurations, which are rarely found in other plasma spray processes, are dependent on a major feature of the induction plasma process; that is, the relatively low in-flight particle velocities.

The pancake-like Al_2O_3 splats produced in the induction plasma process have uniform flat surfaces and near perfect circular circumferences, and attain the *D/d* ratio of ~2.3 to 3.5. The splat thickness is generally ~3 μm, and the ratio of their thickness to span is rarely less than 1:20.

The important factors that control the optimal development of splats (*D/d*) are the spray chamber pressure, the spraying distance, and the spray powder particle size. The interactions between the pressure and other factors are very significant.

With the help of the plasma diagnostic techniques, the surface temperature T_p and velocity U_p of particles prior to impact on the substrate have been measured. To produce pancake-like splats from alumina particles, in the size range –75+63 μm in the induction plasma process, the threshold temperature and particle velocities required are approximately 2300 K < T_p < 2600 K and 20 m/s < U_p < 40 m/s, respectively.

Acknowledgments

The authors thank Dr. Patrick Gougeon for performing the plasma diagnostic for this work. Their colleague, Dr. Peter Lanigan, is acknowledged for his commentary and proof reading of this article.

References

1. J. Madejski, Solidification of Droplets on a Cold Surface, *Int. J. Heat Mass Transfer*, Vol 19, 1976, p 1009-1013
2. A. Vardelle, M. Vardelle, R. McPherson, and P. Fauchais, "Study of the Influence of Particle Temperature and Velocity Distribution within a Plasma Jet Coating Formation," Paper 30, *Proc. of Ninth International Thermal Spraying Conf.*, 19-23 May (The Hague), 1980, p 155-161

3. J.M. Houben, Future Development in Thermal Spraying, *Proc. of the Second American Thermal Spraying Conference,* 31 Oct - 2 Nov 1984, (Long Beach, USA)
4. V.P. Lyaguskin and O.P. Solonenko, Complex Experiment in Plasma Jet Coating Spraying, *High Temperature Dust-Laden Jets in Plasma Technology,* O.P. Solonenko and A.I. Fedorchenko, Ed., Novosibirsk, 1989, p 285-298
5. V.V. Kudinov, P.Yu. Pekshev, and V.A. Safiullin, Forming of the Structure of Plasma-Sprayed Materials, *High Temperature Dust-Laden Jets in Plasma Technology,* O.P. Solonenko and A.I. Fedorchenko, Ed., Novosibirsk, 1989, p 381-418
6. H. Hamatani, T. Okada, and T. Yoshida, "Radio-Frequency and Hybrid Plasma Spraying of Ceramic," ICPS-9, Italy, 1989, p 1527-1532
7. T. Yoshida, T. Okada, H. Hamatani, and H. Kumaoka, Integrated Fabrication Process for Solid Oxide Fuel Cells using Novel Plasma Spraying, *Plasma Sources Sci. Technol.,* Vol 1, 1992, p 195-201L
8. C. Moreau, P. Cielo, and M. Lamontagne, Flattening and Solidification of Thermally Sprayed Particles, *J. Thermal Spray Technol.,* Vol 1 (No. 4), 1992, p 1317-1323
9. L. Bianchi, F. Blein, P. Lucchese, M. Vardelle, A. Vardelle, and P. Fauchais, Effect of Particle Velocity and Substrate Temperature on Alumina and Zirconia Splat Formation, *Thermal Spray Industrial Applications,* C.C. Berndt and S. Sampath, Ed., ASM International, 1994, p 569-574
10. N. Nomoto, K. Kuroda, and T. Yoshida, In-situ Measurement of Rapid Deformation and Solidification Process upon Impact of a Single Sprayed Particle, *Proc. of the Eighth Symposium on Plasma Science for Materials,* Japan Society for the Promotion of Science, Committee 153, 15-16 June 1995 (Tokyo), p 49
11. P. Fauchais, M. Vardelle, A. Vardelle, L. Bianchi, and A.C. Léger, Parameters Controlling the Generation and Properties of Plasma Sprayed Zirconia Coatings, *Plasma Chem. Plasma Process.,* Vol 16 (No. 1) (supplement), 1996, p 99S
12. M. Bussmann, J. Mostaghimi, and S. Chandra, On a Three-Dimensional Model of Droplet Impact, *Proc. of the Third Asia-Pacific Conf. on Plasma Science and Technology,* Japan Society for the Promotion of Science, Committee 153, 15-17 July 1996 (Tokyo), p 95-100
13. O.P. Solonenko and A.V. Smirnov, Generalized Map of the Plasma Sprayed Splats Formation, *Proc. of the Third Asia-Pacific Conf. on Plasma Science and Technology,* Japan Society for the Promotion of Science, Committee 153, 15-17 July 1996, p 247-252
14. A.C. Léger, M. Vardelle, A. Vardelle, P. Fauchais, S. Sampath, C.C. Berndt, and H. Herman, Plasma Sprayed Zirconia: Relationships between Particle Parameters, Splat Formation and Deposit Generation, Part 1: Impact and Solidification, *Thermal Spray: Practical Solutions for Engineering Problems,* C.C. Berndt, Ed., ASM International, 1996, p 623-628
15. M. Pasandideh-Fard and J. Mostaghimi, On the Spreading and Solidification of Molten Particles in a Plasma Spray Process: Effect of Thermal Contact Resistance, *Plasma Chem. Plasma Process.,* Vol 16 (No. 1) (supplement), 1996, p 83S
16. H. Fukanuma, Mathematical Modeling of Flattening Process on Rough Surface in Thermal Spray, *Thermal Spray: Practical Solutions for Engineering Problems,* C.C. Berndt, Ed., ASM International, 1996, p 647-656
17. R. Bhola and S. Chandra, Splat Solidification of Tin Droplets, *Thermal Spray: Practical Solutions for Engineering Problems,* C.C. Berndt, Ed., ASM International, 1996, p 657-663
18. M. Fukumoto, S. Katoh, and I. Okane, "Splat Behavior of Plasma Sprayed Particles on Flat Substrate Surface," *Proc. of ITSC'95,* May 1995, Kobe, p 353-358
19. Y. Huang, M. Ohwatari, and M. Fukumoto, Effect of Substrate Material on Flattening Behavior of Plasma Sprayed Ni Particles, *Proc. of the Sixth Int. Symp.,* Japan Welding Society, Nagoya, 1996, p 731-736
20. W.D. Kingery, H.K. Bowen, and D.R. Uhlmanna, *Introduction to Ceramics,* John Wiley & Sons, 1979
21. D.C. Montgomery, *Design and Analysis of Experiment,* John Wiley & Sons, 1984
22. X. Fan, Induction Plasma Deposition of Alumina Free Standing Parts, Ph.D. thesis, University of Sherbrooke, Canada, 1994
23. T. Okada, H. Hamatani, and T. Yoshida, Radio-Frequency Plasma Spraying of Ceramics, *J. Am. Ceram. Soc.,* Vol 72 (No. 11), 1989, p 2111-2116